1-1-1971

Dimensional Analysis of Seed-Moisture Movement in Deep-Bed Drying

K.S. Chien

R. K. Matthes

B.P. Verma

Dimensional Analysis of Seed-Moisture Movement in Deep-Bed Drying

Kuang S. Chien, R. Kenneth Matthes, Brahm P. Verma
MEMBER ASAE MEMBER ASAE

THIS paper presents the results of an investigation of deep-bed seed drying to develop empirical equations for predicting seed-moisture content in a bin drier.

A number of researchers have set up equations and theory on the mechanisms of moisture flow in seed and grain. However, most of the published works have dealt with thin-layer investigations.

Various aspects of deep-bed drying of seed and grain have been studied from the theoretical standpoint by investigators. By making use of several simplifying assumptions, they based their analysis on the heat and mass balance in a thin layer, considering that a deep bed is the formation of a group of thin layers, and developed calculation formulas layer by layer.

This paper considers an approach to the investigation of the seed-moisture movement in deep-bed drying which includes the use of dimensional analysis. This method of analysis provides a basis for combining several variables which influence the drying phenomenon and enables one to obtain empirical equations.

Objectives

The objectives of this study were:

1 To establish empirical equations for predicting seed-moisture profile of a deepbed at any time during the drying process.

2 To predict the positions of the drying front in deep-bed drying.

Review of Literature

Hukill and Schmidt (8)* stated that the flow of moisture from seed is sometimes considered as analogous to the flow of heat from a body immersed in a cooler fluid. Newton's law of cooling expresses the rate of cooling as proportional to the difference in temperature between the body and the fluid. An analogous expression for moisture flow leads to the conclusion that the rate of moisture loss is proportional to the difference in moisture content between the material being dried and the equilibrium moisture content of the drying air. This may be stated as

$$\frac{dM}{d\Theta} = -k(M-Mc) \quad \ldots \quad [1(a)]$$

or

$$\frac{M-Mc}{Mo-Mc} = a \exp(-k\Theta) \quad . \quad [1(b)]$$

where

M is moisture content, lb water per lb of dry grain
Mc is equilibrium moisture content, lb water per lb dry grain
Mo is initial moisture content, lb water per lb dry grain
Θ is time, hr
k is drying-rate constant (hr^{-1}), and
a is coefficient (intercept on the ordinate of semilog paper).

Equations [1(a)] and or [1(b)] also have been used by other workers as a basic prediction equation in the field of grain drying (1, 2).

In deep-bed drying, the drying rate varies with depth and time. The change in moisture content of the seed at a given depth and at a given time depends upon the character of the seed and the air used for drying. Hukill (7) pointed out that the initial moisture content, the equilibrium moisture content, the characteristics of seed, latent heat of drying of the moisture in the seed, air-flow rate, seed depth, the initial seed temperature, temperature of the drying air and relative humidity may affect the instantaneous moisture content at a certain time after the air flow has started. Some of them are emenable to a considerable degree of control, either in design or operation of the system; however, the variables that depend primarily on the basic physical characteristics of the seed can be controlled only to a minor degree.

Boyce (2) pointed out an important phenomenon in deep-bed drying that, at the beginning of drying, the air temperature throughout the grain mass rapidly changes from the initial grain temperature to the so-called "pseudo-saturation" temperature. Once this temperature has been reached, the heating zone moves upward and, if drying is sufficiently prolonged, the entire batch approaches the drying temperature while the moisture content approaches the equilibrium moisture content.

Previous attempts to develop analytical methods, generally application of the diffusion equation or some form of it, to deep-bed drying have usually been based on the assumption that a deep bed can be regarded as a series of thin beds (1, 2, 6, 15, 16). If it is possible to predict moisture changes

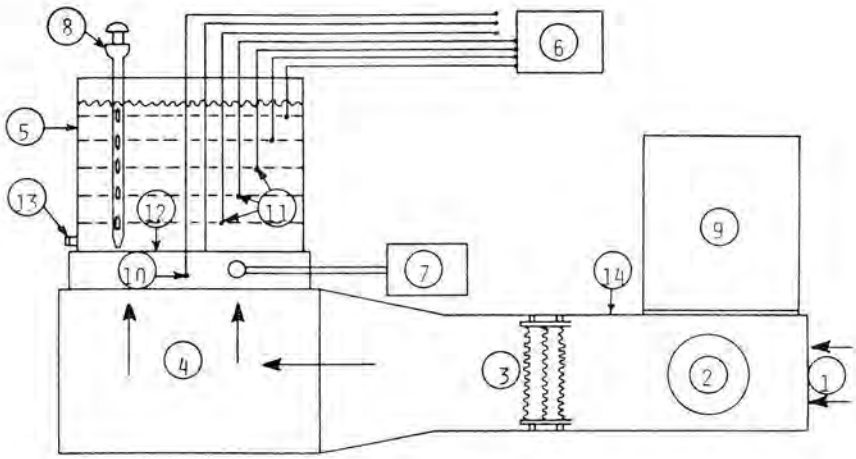

1. AIR INLET
2. VARIABLE SPEED FAN
3. ELECTRIC HEATER
4. PLENUM CHAMBER
5. BIN
6. DIGITAL THERMOMETER
7. VELOMETER
8. SEED TRIER
9. TEMPERATURE CONTROLLING UNIT
10. AIR TEMPERATURE MEASUREMENT
11. THERMISTORS
12. SCREEN WIRE
13. ACCESS HOLE
14. AIR DUCT

FIG. 1 Diagramatic section of apparatus.

Paper No. 69-833 was presented at the Winter Meeting of the American Society of Agricultural Engineers at Chicago, Ill., December 1969, on a program arranged by the Electric Power and Processing Division.

The authors are: KUANG S. CHIEN, reliability engineer, White Motor Co., Chicago, Ill.; R. KENNETH MATTHES, associate professor, agricultural and biological engineering department, Mississippi State University, State College, and BRAHM P. VERMA, assistant agricultural engineer, agricultural engineering department, University of Georgia, Experiment.

* Numbers in parentheses refer to the appended references.

This article is reprinted from the TRANSACTIONS of the ASAE (Vol. 14, No. 2, pp. 277, 278, 279, 280 and 281, 1971)
Published by the American Society of Agricultural Engineers, St. Joseph, Michigan

in a thin bed, then groups of thin layers can be combined to form a deep bed.

Hukill (7) derived a differential equation based on heat balance. He stated that the heat of vaporization of the moisture evaporated from the grain is equal to the sensible heat loss in the air passing through the grain.

Nelson (11) developed an empirical equation based on dimensional analysis and theory of similitude from which the average drying effect by air (pound of moisture removed from batch per pound of dry air circulated) can be predicted.

Dimensional Analysis

In general, the variables which affect the phenomenon of seed drying are of the following three categories: (a) the several linear dimensions fully defining the geometrical boundary conditions, (b) kinetic and dynamic characteristics of flow, and (c) the moisture and thermal status of the seed and air in the system. The variables that were considered pertinent in this study are listed in Table 1.

There are several variables and three basic dimensions involved. Thus from the Buckingham Pi theorem (10) it follows that four Pi terms can be formed. Therefore, an implicit functional relationship involving the Pi terms is

$$MR = f(V\Theta,\ L,\ X/L,\ Ts/Ta) \quad \ldots\ldots\ldots\ldots\ [2]$$

For simplicity, the following notations were used in this study:

$$\frac{M - Me}{Mo - Me} = MR \qquad \text{Moisture ratio}$$

$$\frac{V\Theta}{L} = \Theta^{\circ} \qquad \text{Time factor}$$

$$\frac{X}{L} = X^{\circ} \qquad \text{Depth ratio}$$

$$\frac{Ts}{Ta} = T^{\circ} \qquad \text{Temperature ratio}$$

Therefore, equation [2] becomes

$$MR = f(\Theta^{\circ},\ X^{\circ},\ T^{\circ}) \quad \ldots\ldots\ [3]$$

Apparatus and Procedure

The experimental seed drier was constructed by Lennox Industries, Inc., and rebuilt for modeling deep-bed drying studies of freshly harvested rice seed. Fig. 1 shows the drying bin, labeled as part 5, used in the experiment. The bin was 16 in. in diameter and 16 in. deep.

Fresh air was admitted at 1, passed through the metallic duct (14) via the fan (2), which was driven through a variable-speed arrangement for air to be supplied at various rates. In passing through the heating unit (3) the air temperature was raised to the desired level and a manually controlled heating arrangement (9) maintained the desired temperature within + 1 F range. The heated air entered the air chamber (4), passed through the screen (12) and through the seed mass, where temperatures within the bed could be measured at 2.8-in. intervals from the bottom by temperature sensors connected to a digital thermometer (6) with four switches to select the depth at which the temperature measurement was desired.

During the test, initial seed beds 14 and 15 inches deep were used. A 0.5 in. diameter seed trier (8) with partitions between openings was used to obtain the samples at 2.8-in. intervals from the bottom up to 14 in. Samples of the bottom layer were obtained from a one-inch access hole (13) on the bin side just above the bottom. A rubber stopper was used to seal off the air during drying trials. For the 15-in. seedbed, an approximate 1.5 inches reduction of seed depth was observed after ten hr drying due to shrinkage, sample removal, and seed probe disturbances during sample removal. Therefore, all analyses were based on a seed depth of 14 in.

The time intervals in getting seed samples for the moisture test and temperature readings of the seeds were 1 hr between readings for the first 6 hr, then 2-hr intervals until the desired dryness was obtained (usually 10 to 12 hr).

The air temperature, air-flow rate, and initial seed-moisture content were varied in the tests. For each test, a constant level of these variables were selected. The schedule of six test runs is shown in Table 2.

The pseudo-saturation temperatures (*Ts*) were taken at 11.2 and 14-in. depths 30 min to 1 hr after drying commenced. As shown by Boyce (2), at the beginning of drying the air temperature throughout the grain mass rapidly changes from the initial grain temperature (*To*) to the pseudo-saturation temperature. It remained at this temperature until the drying front reached this depth. This is seen in Fig. 3.

Samples of seed were removed during runs at each level and were used to determine moisture content.

Analysis and Interpretation of Results

A series of tests were made with different drying conditions. In each test, the air temperature, air-flow rate, and seed depth were kept constant (neglecting the shrinkage effect). Typical results of deep bed tests are shown in Figs. 2 and 3.

Fig. 2 shows the moisture profiles during a drying test with initial moisture content of 26 percent d.b., using 17.3 ft per min air flow at 85 F. Moisture contents of seed at six different depths in a 15-in. bed are shown in Fig. 2, where the lowest curve representing the bottom of the bed is analogous to a thin-bed curve. The drying front reached the 2.8-in. level immediately after the start of drying. At

TABLE 1. PERTINENT VARIABLES FOR SEED DRYING

No.	Symbol	Description	Units	Dimensions*
1	MR	Moisture ratio $\frac{M - Me}{Mo - Me}$		
		M = Instantaneous moisture content	lb water per lb seed	
		Mo = Initial moisture content	lb water per lb seed	
		Me = Equilibrium moisture content	lb water per lb seed	
2	L	Total depth of seed	ft	L
3	X	Depth from the bottom	ft	L
4	V	Air-flow rate	ft per min	L(-)$^{-1}$
5	(-)	Time of drying	hr	(-)
6	Ta	Temperature of drying air	deg F	T
7	Ts	Pseudosaturation temperature	deg F	T

*Fundamental dimensions selected were length, time and temperature (L, (-), T).
Temperature in degrees Rankine (R).

TABLE 2. DETAILS OF DEEP-BED INVESTIGATION OF RICE.

Run No.	Initial seed temp., deg F	Initial seed depth, in.	Air conditions: Drying air temp., deg F	Air conditions: Pseudo-saturation temp., deg F	Air conditions: Air flow ft per min	Air conditions: Relative humidity, percent	Seed moisture content percent d.b.: Initial	Seed moisture content percent d.b.: Equilibrium
1	69.3	15	85	66.0	17.3	33	26.0	8.0
2	70.0	15	90	62.5	23.0	30	24.5	7.5
3	70.7	15	95	70.0	17.3	30	27.2	6.5
4	64.4	15	100	66.0	19.0	33	24.5	6.5
5	60.5	15	110	68.0	20.0	25	24.5	5.0
6	72.3	14	111	79.0	24.0	20	22.8	4.8

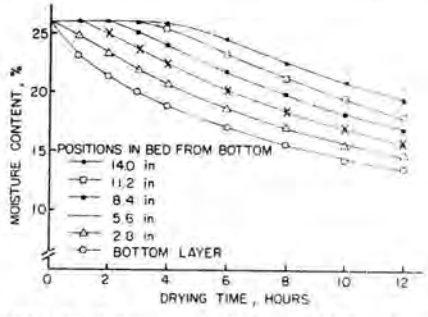

FIG. 2 Moisture profile in a 15-in. deep bed at drying-air temperature of 85 F. (Airflow rate, 17.3 ft per min).

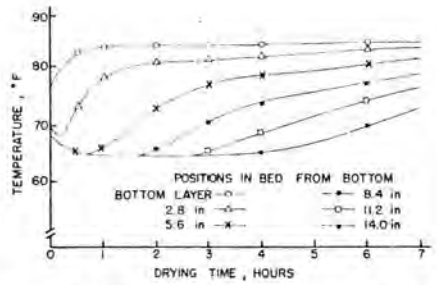

FIG. 3 Temperature profile in a 15-in. deep bed at drying-air temperature of 85 F.

the 5.6, 8.4, 11.2 and 14-in. levels, the moisture contents began to decrease after 1, 2, 3, and 4.5 hr of drying, respectively. Therefore, the progress of the so-called drying front can be seen from Fig. 2 by noticing the level at which the drying actually begins.

Fig. 3 shows the temperature profile during the same drying test. The temperature of the seed at the bottom increased to the drying-air temperature. The temperature at the upper layers decreased from the initial seed temperature to the pseudo-saturation temperature immediately after the start of drying and remained almost constant until the drying front reached that depth. Similar phenomenon occurred in another test at air temperature of 110 F and 20.0 ft per min of air-flow rate, except that the pseudo-saturation temperature, Ts, was higher than that of the initial seed temperature, To, and the drying front traveled faster than that observed for the 85 F test. The detail results are presented by Chien (3).

Data from Fig. 2 were plotted on semilog coordinates with the dimensionless moisture ratio, MR, against time factor, $\Theta°$, for the 85 F test (Fig. 4). Similar plots of other tests were made. A family of straight lines were observed for each level of depth ratio, $X°$; however, at MR values close to unity, this was not true. The extension of each straight line of the plots of MR versus $\Theta°$ was made to obtain the intercept.

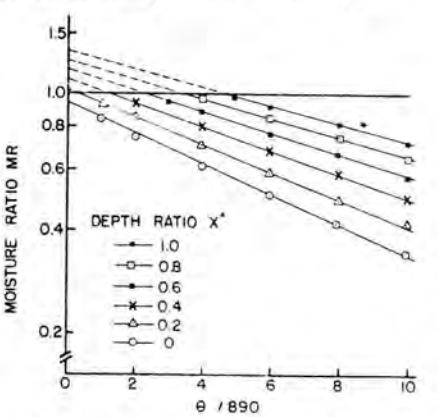

FIG. 4 Semilogarithmic plots of moisture ratio as a function of time factor for various values of depth ratio at drying-air temperature of 85 F.

The general form of the equation of the family of straight lines of the plots of MR versus $\Theta°$ (See sample Fig. 4) is:

$$\ln MR = f(X°)\,\Theta° + f_2(X°) \quad \ldots\ldots\ldots\ldots [4(a)]$$

or

$$MR = \exp\,[f_1(X°)\,\Theta° + f_2(X°)] \quad \ldots\ldots [4(b)]$$

where

$f_1(X°)$ = slopes of the lines in plots of MR versus $\Theta°$ which is a function of depth ratio $(X°)$

$f_2(X°)$ = intercepts of the lines in the plots of MR versus $\Theta°$ which is a function of depth ratio $(X°)$.

To investigate the nature of functions of $f_1(X°)$ and $f_2(X°)$, the slopes and intercepts of the lines in Fig. 4 were calculated and then plotted against the depth ratio, $X°$, as shown

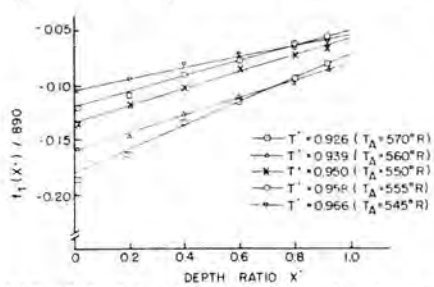

FIG. 5 $F_1(X°)$ versus depth ratio at various values of temperature ratio.

in Figs. 5 and 6, where five different test runs are shown. Since $f_1(X°)$ and $f_2(X°)$ are linear with depth ratio, $X°$, the following mathematical models were fitted:

$$f_1(X°) = A + BX° \quad \ldots\ldots [5]$$

and

$$f_2(X°) = C + DX° \quad \ldots\ldots [6]$$

where A, B, C, and D are coefficients. The substitution of equations [5] and [6] into [4b] yields

$$MR = \exp\,[(A + BX°)\,\Theta° + (C + DX°)], \text{ for } MR = 1 \ldots [7]$$

At a constant drying temperature, equation [7] fits the data well in each test run.

The coefficients A, B, C, and D in equation [7] are functions of the temperature ratio, $T°$, that is, the values of these coefficients change as the temperature ratio is changed. To determine the nature of the relationship between the coefficients and the temperature ratio, values of $A(T°)$, $B(T°)$, $C(T°)$, and $D(T°)$ were determined from Figs. 7, 8, 9, and 10. These values of the coefficients were plotted on rectilinear coordinates. Again, linear relationships were obtained and

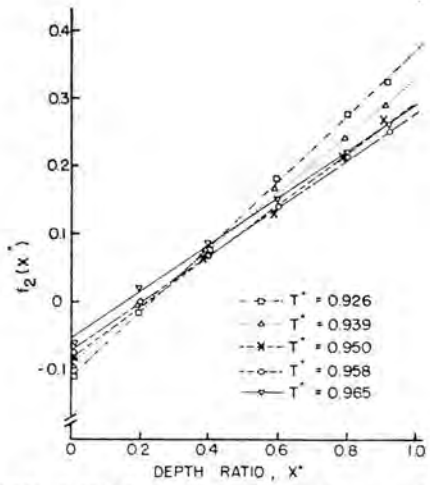

FIG. 6 $F_2(X°)$ versus depth ratio at various values of temperature ratios.

the following mathematical models were fitted:

$$A(T°) = A_1 + A_2T° \quad \ldots\ldots [8]$$

$$B(T°) = B_1 + B_2T° \quad \ldots\ldots [9]$$

$$C(T°) = C_1 + C_2T°, \text{ and} \quad \ldots [10]$$

$$D(T°) = D_1 + D_2T° \quad \ldots\ldots [11]$$

The substitution of [8], [9], [10] and [11] into [7] gives

$$MR = \exp\,\{[A_1 + A_2T° + (B_1 + B_2T°)X°]\Theta° + C_1 + C_2T° + (D_1 + D_2T°)X°\},$$

$$\text{for } MR = 1 \quad \ldots\ldots [12]$$

The original form of the prediction equation and its restriction is

$$\frac{M - Me}{Mo - Me} = \exp\left\{\left[A_1 + A_2\frac{Ts}{Ta} + \left(B_1 + B_2\frac{Ts}{Ta}\right)\frac{X}{L}\right]\left(\frac{V\Theta}{L}\right) + C_1 + C_2\frac{Ts}{Ta} + \left(D_1 + D_2\frac{Ts}{Ta}\right)\frac{X}{L}\right\} \quad \ldots\ldots [13]$$

for

$$\frac{M - Me}{Mo - Me} = 1.$$

From the regression analysis of data, the following values were obtained for the coefficients:

$A_1 = -0.002204$
$B_1 = 0.001549$
$C_1 = -1.4802$
$D_1 = 4.0576$
$A_2 = 0.002160$
$B_2 = 0.002160$

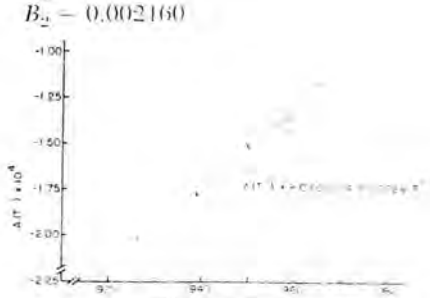

FIG. 7 Plot of A(T°) versus T°.

$C_2 = 1.4759$
$D_2 = 3.8610$

Comparison of Predicted and Measured Moisture Profiles

A graphical comparison of predicted and measured moisture profiles for test No. 6 (111 F air temperature, 24.0 ft per min air flow rate and 14 in. initial seed depth) is shown in Fig. 11.

It should be noted that equations [7] and [13] are subject to the restriction, $MR \leq 1$. It is possible to have the moisture content greater than the initial moisture content after a certain length of drying time due to the cold seed present in the upper layer and or non-uniform initial moisture content. However, the study of this effect is not within the scope of the present study. This assumption leads to the conclusion that the computed values of MR greater than unity should be rejected, and the moisture content of that layer should be considered at the initial moisture content.

Values of MR equal to unity show the position the drying front reaches at a certain time after drying. From then on, the moisture content begins to decrease at that layer.

In the prediction equation [13] initial and equilibrium moisture contents, seed depth, air-flow rate, air temperature and elapsed time are known before the test. However, as mentioned before, the pseudo-saturation temperatures were found after 30 minutes to one hour of drying at the upper layers of seed, where temperature remained constant. In the selection of the pertinent variables, it was assumed that the pseudo-saturation temperature was a function of initial seed moisture content and relative humidity. This means that the relative humidity is implicit in the pseudo-saturation temperatures.

Equation [13] may be arranged:

$$\frac{M-Me}{Mo-Me} = \exp\left[\left(\frac{V\Theta}{L}\right) f_1 + f_2\right] = \exp\left(\frac{V\Theta}{L}\right) f_1 \exp\,(f_2)$$

$$= F_2 \exp\left[\left(\frac{V\Theta}{L}\right) f_1\right] \qquad \ldots\ldots\ldots\ldots\ldots\ldots\ldots\ldots [14]$$

where

$$f_1 = A_1 + A_2\left(\frac{Ts}{Ta}\right) + \left[B_1 + B_2\left(\frac{Ts}{Ta}\right)\right]\frac{X}{L} \qquad F_2 = \exp\,(f_2) =$$

$$\exp\left[C_1 + C_2\left(\frac{Ts}{Ta}\right) + \left[D_1 + D_2\left(\frac{Ts}{Ta}\right)\right]\frac{X}{L}\right]$$

and other symbols as previously defined. When $(M-Me)\,(Mo-Me)$ is plotted against $(V\Theta\ L)$ on semilog coordinates, it can be seen that f_1 is the function of the slopes of a family of straight lines representing different layers, whereas F_2 is the function of the intercepts of a family of lines representing the corresponding layers.

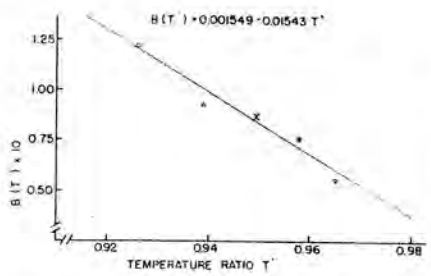

FIG. 8 Plot of B(T°) versus T°.

As previously mentioned, the theoretical analyses of deep-bed drying were usually based on heat and mass balance for each thin layer, and the basic prediction equation [2b] was used. Then layer by layer calculations of the drying conditions through each layer were made to obtain the instantaneous moisture content. In effect, their efforts were to correlate the drying conditions at each layer with drying rate coefficient k and intercept a in equations [1a] and [1b].

The terms f_1 and F_2 in the developed prediction equation [14] took into account various drying conditions for each layer. The desired values of instantaneous moisture content could be easily obtained from this prediction equation.

The drying rate of each layer in a deep bed could be obtained by differentiating the prediction equation [14] with respect to the drying time:

$$\frac{dM}{d\Theta} = (Mo-Me)\left(\frac{V}{L}\right) f_1 \exp\left[\left(\frac{V\Theta}{L}\right) f_1 + f_2\right] \qquad \ldots\ldots\ldots [15]$$

It should be noted that the air-flow rate, air temperature and seed depth were assumed to be constant during the drying operation and that the restriction $MR \leq 1$ prevailed.

Summary and Conclusions

An experimental drier was designed in which deep-bed drying of freshly harvested rice seed at various drying conditions was studied. Six thermistors evenly spaced along the bin axis from the bottom up to the top layer of seed allowed the temperature readings in the seed mass during the drying process. The pseudo-saturation temperature was obtained when the temperature remained constant at upper layers of the seed nearly one hour after the start of drying.

This study was conducted using various levels of air-flow rates in the range of 17.3 to 24.0 ft per min., with various drying air temperatures ranging from 85 to 111 F (545-571 R) and initial seed moisture contents of 22.8 to 27.2 percent, dry basis. Using initial seed depths of 14 and 15 in., the seed moisture was measured at depths of 0, 2.8, 5.6, 8.4, 11.2 and 14 in. (depth measured from the bottom).

Dimensional analysis with experimentation provided a prediction equation describing moisture profiles for deep-bed drying.

Based on the assumptions and analysis described above, and within the test range of each variable, the following conclusions were made:

(1) At a constant drying temperature, the following equation describes the moisture profile in deep-bed drying:

$$\frac{M-Me}{Mo-Me} = \exp\left[\left(A+B\frac{X}{L}\right)\left(\frac{V\Theta}{L}\right) + C + D\frac{X}{L}\right] \quad \text{for} \quad \frac{M-Me}{Mo-Me} = 1$$

where A, B, C and D are coefficients dependent on temperature ratio, $T°$ Ts Ta,

Ts = pseudo-saturation temperature, R
Ta = temperature of drying air, R
M = instantaneous moisture content
Me = equilibrium moisture content
Mo = initial moisture content

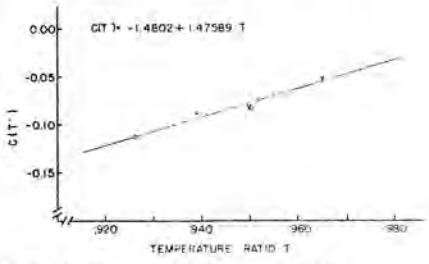

FIG. 9 Plot of C(T°) versus T°.

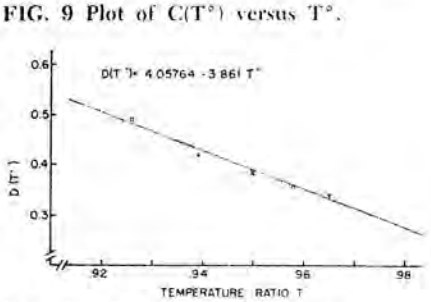

FIG. 10 Plot of D(T°) versus T°.

V = airflow rate
Θ = time
L = total depth of seed, and
X = distance measured from the bottom

(2) At different levels of drying temperature, the equation obtained for predicting the instantaneous moisture content at any depth of seed was:

$$\frac{M - Me}{Mo - Me} = \exp\left[f_1\left(\frac{V\Theta}{L}\right) + f_2\right], \text{ for } \frac{M - Me}{Mo - Me} = 1$$

where

$$f_1 = A_1 + A_2\left(\frac{Ts}{Ta}\right) + \left[B_1 + B_2\left(\frac{Ts}{Ta}\right)\right]\frac{X}{L}$$

$$f_2 = C_1 + C_2\left(\frac{Ts}{Ta}\right) + \left[D_1 + D_2\left(\frac{Ts}{Ta}\right)\right]\frac{X}{L} \quad \text{and}$$

A_1, A_2, B_1, B_2, C_1, C_2, D_1 and D_2 are coefficients.

(3) The criterion of locating the drying front was to determine the closest level from the bottom at which the moisture ratio was equal to unity. This determination can be made by the prediction equation developed in this study.

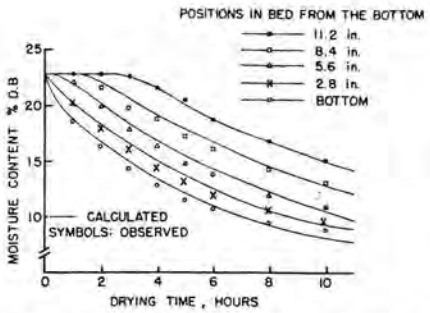

FIG. 11 Comparison of predicted and observed moisture profiles. Drying air temperature: 111 F; air-flow rate: 24 ft per min.; initial speed depth: 14 in.

References

1 Allen, J. R. Application of grain drying theory to the drying of maize and rice. Journal of Agricultural Engineering Research 5:(4)363, 1960.

2 Boyce, D. S. Grain moisture and temperature changes with position and time during thorough drying. Journal of Agricultural Engineering Research 10:(4)333-341, 1965.

3 Chien, K. S. Dimensional analysis of seed moisture movement in deep-bed drying. Unpublished M.S. Thesis. Mississippi State University Library, January 1969.

4 Haynes, B. C., Jr. Vapor pressure determination of seed hygroscopiococy. Technical Bulletin No. 1229 ARS, USDA, Jan. 1961. (Also in "Hygroscopicity of Seeds," **Agricultural Engineers Yearbook** 285-286.

5 Henderson, S. M. and Pabis, S. Grain drying theory: 1. Temperature effect on drying coefficient. Journal of Agricultural Engineering Research 6:(3)169, 1961.

6 Henderson, S. M. and Perry, R. L. Agricultural process engineering. John Wiley and Sons, New York, 1955.

7 Hukill, W. V. Basic principles in drying corn and grain sorghum. **Agricultural Engineering** 28:(8)335-338, 340. August, 1947. (Also in Anderson, J. A. and Alcock, A. W. Storage of cereal grains and their products. American Association of Cereal Chemists, St. Paul, Minn., 1954.

8 Hukill, W. V. and Schmidt, J. L. Drying rate of fully exposed grain kernels. **Transactions of the ASAE** 3:(2)71-80, 1960.

9 Hustrulid, A. and Flikke, A. M. Theoretical drying curve for shell corn." **Transaction of the ASAE** 2:(1)112-114, 1959.

10 Murphy, G. Similitude in engineering. The Ronald Press, New York, 1950.

11 Nelson, G. L. A new analysis of batch grain-drier performance. **Transactions of the ASAE** 3:(2)81-88, 1960.

12 Newman, A. B. Applying diffusion calculations to drying porous solids. Chemical and Metallurgical Engineering 38:(12)710, 1931.

13 Shedd, C. K. Resistance of grains and seeds. **Agricultural Engineers Yearbook**. 267, 1966.

14 Simmonds, K. H. C., Ward, G. T., and McEwen, E. The drying of wheat grain. II. Thorough-drying of deep beds. Transactions of Institute of Chemical Engineers 31:279-288, 1953 (England).

15 Thompson, T. L., Peart, R. M. and Hester, G. H. Mathematical simulation of corn drying—a new model. **Transactions of the ASAE** 11:(4)582-586, 1968.